Size Effects and Odd-Even Effects of Hydrogen Adsorption in Janus MoSSe Nanosheet: First-Principles Studies

Journal:	*Molecular Systems Design & Engineering*
Manuscript ID	ME-ART-01-2020-000014.R1
Article Type:	Paper
Date Submitted by the Author:	26-Feb-2020
Complete List of Authors:	Joo, Paul; University of California San Diego, Department of NanoEngineering Zhang, Jingning; University of California San Diego Yang, Kesong; University of California San Diego, NanoEngineering

Design, System, Application Statement

The symmetry breaking in the two-dimensional (2D) Janus molybdenum chalcogenides offers promising properties for various technological applications, particularly for catalytic applications including hydrodesulfurization and hydrogen evolution reactions, in which the hydrogen adsorption is one critical step determining the catalytic efficiency. Here, we reported nanosize effects of triangular Janus MoSSe monolayer nanostructures by studying their energetic properties and hydrogen adsorption. The Janus MoSSe monolayer structure is found energetically more favorable than the well-studied molybdenum sulfide, MoS2. The calculated changes of Gibbs free energy for hydrogen adsorption on the Se layer are much closer to zero than that on the S layer, implying a better catalytic activity. Interestingly, an obvious odd-even effect on the hydrogen adsorption of the Janus MoSSe nanosheet structures is found. This work provides some useful insights into the design of high-performance Janus MoSSe nanocatalysts.

Size Effects and Odd-Even Effects of Hydrogen Adsorption in Janus MoSSe Nanosheets: First-Principles Studies

Paul H. Joo,[a,b‡] **Jingning Zhang**[b‡] **and Kesong Yang**[*a,b]

Received Xth XXXXXXXXXX 20XX, Accepted Xth XXXXXXXXX 20XX
First published on the web Xth XXXXXXXXXX 200X
DOI: 10.1039/b000000x

The nanosheets of molybdenum dichalcogenides have been widely explored for their catalytic applications including hydrodesulfurization and hydrogen evolution reactions, in which the adsorption of hydrogen plays a key role in determining the catalytic efficiency. Herein, we studied nanosize effects of the triangular Janus MoSSe nanosheets as well as odd-even effects on the hydrogen adsorption using first-principles calculations. It is found that, after structural relaxation, the Janus MoSSe nanosheets form an arch structure with a bend toward S layer because of the structural asymmetry, which is unlike the case of molybdenum sulfide, MoS_2. Moreover, the calculated changes of Gibbs free energy for the hydrogen adsorption exhibits an odd-even oscillation as the size number (n) of the nanosheets changes from odd number to even number. These results highlight the unique structural and catalytic properties of the two-dimensional Janus transition-metal chalcogenides nanostructures.

1 Introduction

The two-dimensional Janus molybdenum chalcogenides show promising properties for various technological applications because of their asymmetrical structures as compared to the symmetrical molybdenum dichalcogenides MoX_2 (X = S, Se, or Te).[1–16] To be specific, the Janus molybdenum chalcogenides have a general formula MoXY (X/Y = S, Se, and Te, X $\neq$ Y) which breaks the mirror symmetry and thus results in a vertical dipole.[16] This unique property makes this class of materials hold great potential for various device applications such as piezoelectric,[1,2] catalytic,[3–9] spintronic,[10,11] and efficient energy harvesting applications.[12,13] In particular, catalytic properties of Janus MoXY are being extensively explored,[3–9] since its parent compound MoS_2 is a well-known catalyst for hydrogen evolution reaction (HER) and hydrodesulfurization.[17–21] A typical example of Janus monolayer MoXY is MoSSe, which has been recently synthesized via sulfurization of monolayer $MoSe_2$[14] and a combinatorial hydrogen plasma treatment and subsequent thermal selenization on monolayer MoS_2.[15] In the first approach,[14] the top layer of Se atoms are substituted by sulfur atoms while the bottom Se layer remains intact. In the second approach,[15] the monolayer MoS_2 was first prepared on sapphire substrate using chemical vapor deposition, and then the top-layer S atoms were replaced with H atoms using the hydrogen plasma; after that, all the H atoms were further replaced with Se atoms via thermal selenization.

A number of research efforts are being made to study their intrinsic electronic,[16,22,23] optical,[8,24] and magnetic properties[10,11] or to identify catalytic active sites for HER[4,9] It is well-known that the parent compound of Janus MoSSe, *i.e.*, MoS_2, can stabilize as monolayers in the catalytic environment,[25,26] and the monolayer MoS_2 nanostructures can exist in multiple shapes, including the triangular shape under the sulfur-rich growth condition.[18,20,27–29] The monolayer Mo_2 nanoclusters could be synthesized on the Au (111) substrate using physical vapor deposition approach, in which the Au substrate acts as a template to disperse Mo into small islands.[27,28] The substrate was then annealed in the sulphiding atmosphere, promoting the sulfidation of Mo islands into

[a]*Program of Materials Science and Engineering, University of California San Diego, La Jolla, CA 92093-0418, USA.*
[b]*Department of NanoEngineering and Program of Chemical Engineering, University of California, San Diego, La Jolla, CA 92093-0448, USA.*
[*]*Tel: +1-858-534-2514; E-mail: kesong@ucsd.edu*
[‡]These authors contributed equally to this work.

MoS_2 nanoclusters. Accordingly, the size of synthesized Mo_2 nanoclusters could be controlled by the size of deposited Mo islands and estimated by measuring the area of the nanoclusters in large-scale scanning tunnelling microscope images.

Our prior first-principles computational studies show that MoS_2 nanosheets exhibit obvious size effects and odd-even effects on the formation of sulfur dimer vacancies in terms of the size of nanosheets (defined as the number of Mo atoms on the edge).[20] Consequently, one may speculate whether Janus MoSSe nanosheets may also exhibit nanosize effects. In particular, it is of interests to know whether the hydrogen adsorption on these nanosheets has such effects since hydrogen adsorption is one critical step in many catalytic reactions including hydrodesulfurization and hydrogen evolution process. Therefore, a computational and theoretical exploration of such effects is necessary to develop a fundamental and comprehensive understanding of the materials properties of Janus MoSSe nanomaterials.

In this article, we explored size effects and odd-even effects on the hydrogen adsorption in the triangular Janus MoSSe nanosheets using first-principles calculations. It is found that, unlike the symmetrical MoS_2, the relaxed Janus MoSSe nanosheets exhibit an arch structure with a bend toward S layer because of the broken mirror symmetry. The calculated changes of Gibbs free energy for the hydrogen adsorption exhibits an odd-even oscillation as the size number (n) of the nanosheets changes. This work reminds the unique structural and catalytic properties of the two-dimensional Janus transition-metal chalcogenides nanostructures.

2 Computational Details

First-principles density functional theory (DFT) calculations were performed using Vienna Ab-initio Simulation Package (VASP).[30,31] The Projector-Augmented Wave (PAW) potential was employed for the treatment of the electron-ion interactions[32] and the Generalized Gradient Approximation (GGA) parameterized by Perdew-Burke-Ernzerhof (PBE) was used for electron exchange-correlation functional.[33] A single Γ point was used in our calculations with a cut-off energy of 310 eV that was set as the 1.2 times of the default maximum cut-off energy of the pseudopotentials after convergence test calculations.

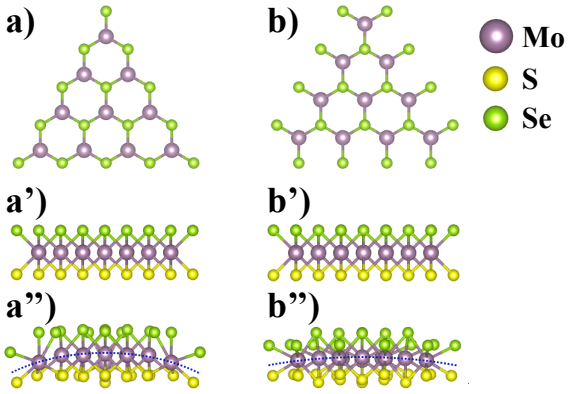

Fig. 1 Janus monolayer MoSSe nanosheets (n = 4) with zig-zag patterned edges from top view (a-b), side view (a'-b'), and side view after structural relaxation (a"-b") , respectively. (a, a', a") ZZ-S1, (b, b', b") ZZ-S2. The purple, yellow, and green balls represent Mo, S, and Se atoms, respectively. The size of the nanosheet (n) is indicated by the number of Mo atoms in the edge of the MoSSe nanosheet.

All the atomic positions of the Janus MoXY nanosheets were relaxed until all components of the residual forces were less than 0.02 eV/Å and the tolerance of convergence for the self-consistent-field iteration was set to 10^{-5} eV.

3 Results and Discussion

3.1 Formation Energy

In this work, two types of triangle MoSSe nanosheets with zig-zag patterned and chalcogen-atom-terminated edges were considered, as shown in Figure 1. The Janus MoSSe nanosheet models were built by replacing one layer of S atoms with Se atoms on the basis of the MoS_2 nanosheet structures. By following our previous naming convention,[20] these two edge structures were defined as ZZ-S1 and ZZ-S2, respectively. The size of the MoSSe nanosheets is defined by the number of Mo atoms on the edge, indicated by a variable n. Figure 1 shows two example MoSSe nanosheets both having a size number of n = 4. After structural relaxation, interestingly, the two types of MoSSe nanosheets both exhibit an arch structure with apex toward Se layers, and the degree of the curvature of the ZZ-S1 type is larger than that of ZZ-S2 type, see Figure 1a" and 1b". This phenomenon is different from the case of MoS_2 nanosheets in which the

two S layers are symmetrical to the Mo layer and the Mo layer is flat after structural relaxation. The formation of the arch structure in the Janus MoSSe nanosheets can, therefore, be explained from the asymmetrical S and Se layers that are both connected to the Mo layer. To be specific, the S-layer has a much stronger attraction to the Mo atoms than the Se-layer because of the shorter and stronger S-Mo bond than Se-Mo bond, thus leading to the bending of Mo layers toward S layer.

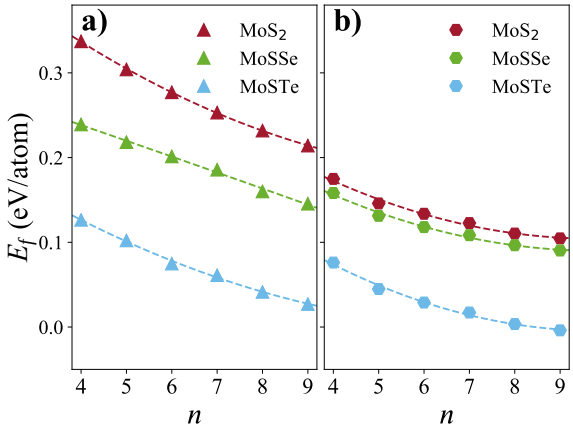

Fig. 2 Calculated formation energies of a) ZZ-S1 and b) ZZ-S2 models of MoS_2 (red), MoSSe (green), and MoSTe (cyan) nanosheets, with respect to the size (n).

To evaluate the structural stability of the MoSSe nanosheets, we calculated their formation energies using the following equation:

$$E_f = [E_{total} - zE_{MoSSe} - (x-z)\mu_S - (y-z)\mu_{Se}]/(x+y+z) \quad (1)$$

where E_{total} is the total energy of the MoSSe nanosheet, E_{MoXY} is the total energy of the bulk MoSSe, μ_X and μ_Y are the chemical potentials of S and Se atoms, respectively, and x, y, and z is the number of S, Se, and Mo atoms, respectively.

The calculated formation energies with respect to the size (n) are plotted in Figure 2. To have a comprehensive comparison, the formation energies of MoS_2 and Janus MoSTe nanosheets were also calculated and plotted in the figure. Our calculations reveal the following trends:

i) As the size (n) of Janus MoSSe and MoSTe nanosheets increases, the formation energy of the two types of triangular nanosheets decreases, suggesting that the larger Janus MoSSe and MoSeTe nanosheets are energetically more favorable to form, similar to the case of MoS_2 nanosheets.[20]

ii) At the same size (n), the ZZ-S2 model has a lower formation energy than ZZ-S1 model for the Janus MoSSe and MoSTe structures, implying that the ZZ-S2 structures are energetically more favorable to form in practical. This is also similar to the case of MoS_2 in which this phenomenon has been validated in the experiment.[18]

iii) At the same size (n), the calculated formation energy of the three types of nanosheet structures follows the order $MoS_2 > MoSSe > MoSTe$. This indicates that the Janus MoSSe is energetically more favorable to form than the MoS_2 while the MoSTe is the energetically most favorable to form.

3.2 Hydrogen Adsorption Energy

To explore nanosize effects on the catalytic performance in the Janus MoSSe nanosheets, herein we investigated the hydrogen adsorption on the Janus MoSSe nanosheets. This is because the hydrogen adsorption on the active sites is one critical step in both hydrodesulfurization catalytic reaction and hydrogen evolution process. In these reaction processes, hydrogen-adsorbed MoSSe nanosheets (H^*-MoSSe) act as an intermediate state, thus being responsible for the catalytic activity.

In principle, one hydrogen atom (H^+) can be adsorbed to either S layer or Se layer of MoSSe. However, it is noted that one necessary criterion for a material to be a good catalyst is that the changes of Gibbs free energy for hydrogen adsorption is close to zero, *i.e.*, $\Delta G_H = 0$.[34] One can generally infer that H-adsorption on the S layer has a more negative value of ΔG_H than that on the Se layer because of higher electron negativity of S, which makes it difficult for the H to be desorbed from the S site. As discussed later, this conclusion can be confirmed from our first-principles calculations. Hence, to identify the energetically preferred catalytic active sites for hydrogen adsorption in the Janus MoSSe, herein we firstly discussed H-adsorption on the Se layer of the MoSSe nanosheets. The ZZ-S1 and ZZ-S2 models of the Janus MoSSe nanosheets with $n = 4$ and 5 were selected as representatives, and one hydrogen atom was added on each of the different Se-sites based on the geometrical symmetry.

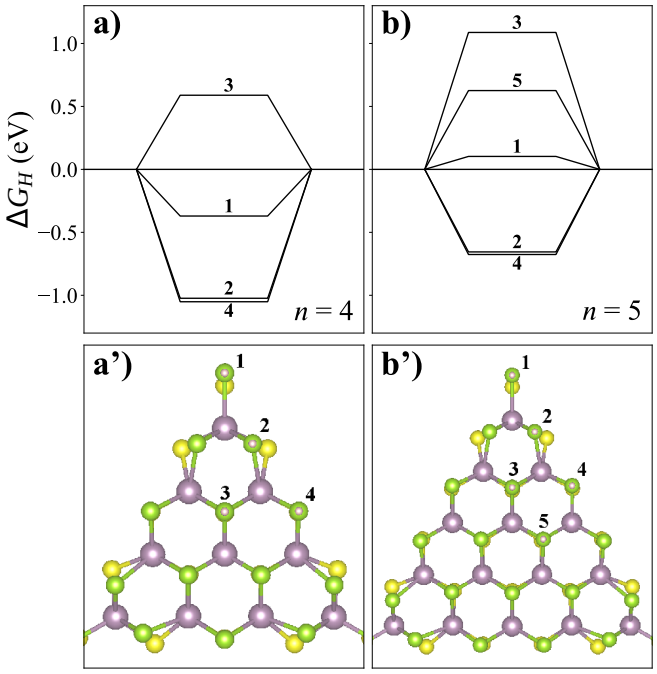

Fig. 3 a-b) Calculated changes of hydrogen Gibbs free energies (ΔG_H) with respect to the different H-adsorption sites of ZZ-S1 MoSSe nanosheets for n = 4 and 5, respectively. a'-b') The geometrical display of the H-adsorption sites H@Se for n = 4 and 5, respectively.

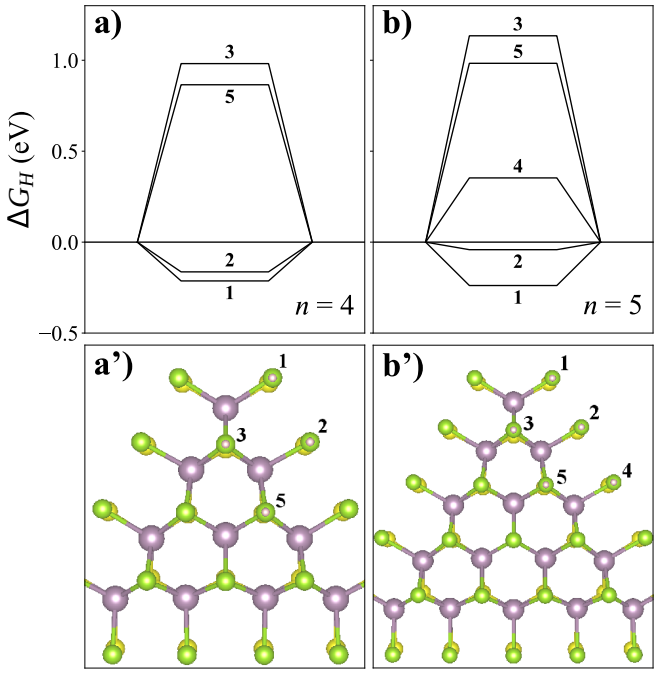

Fig. 4 a-b) Calculated changes of hydrogen Gibbs free energies (ΔG_H) with respect to the different H-adsorption sites of ZZ-S2 MoSSe nanosheets for n = 4 and 5, respectively. a'-b') The geometrical display of the H-adsorption sites H@Se for n = 4 and 5, respectively.

The change of the Gibbs free energy of the hydrogen adsorption on the MoSSe nanosheets was then calculated using the following equation:

$$\Delta G_H = \Delta E_H + \Delta E_{ZPE}(H) - T\Delta S_H \qquad (2)$$

where ΔE_H is the difference in the total energy between H*-MoSSe and unbound hydrogen atom and MoSSe nanosheet, and $\Delta E_{ZPE}(H)$ and ΔS_H are the difference of zero-point energy and the difference of entropy for the hydrogen atom, respectively, between its adsorbed states and the isolated states. The value of 0.41 eV for $T\Delta S_H$ was taken from previous literature at T = 300K.[4]

The calculated ΔG_H for the H-adsorption on each of the possible Se sites are shown in Figure 3 for ZZ-S1 model and in Figure 4 for ZZ-S2 model, respectively. In both Figure 3 and Figure 4, a) and b) represent the plotted ΔG_H with respect to the H-adsorption sites, while a') and b') show the geometrical representation of the H-adsorption at each site for n = 4 and 5, respectively. Based on the calculation results, the followings conclusions can be revealed:

(i) For both ZZ-S1 and ZZ-S2 models, the H-adsorption sites near the center of the nanosheet such as sites 3 and 5 lead to a relatively large positive value of ΔG_H, which means that the hydrogen atoms are less likely to be adsorbed on these sites.

(ii) For the ZZ-S1 model, the H-adsorption on the edges such as sites 2 and 4 leads to a relatively larger negative value of ΔG_H, indicating a spontaneous H-adsorption process and thus, more difficult for the H atoms to be desorbed; the H-adsorption at the corner site, *i.e.*, site 1, results in a ΔG_H that is the closest to zero, implying the best catalytic behavior.

(iii) For the ZZ-S2 model, the H-adsorption at the corner edge sites 1 and 2 has a negative ΔG_H, with the site 2 having the ΔG_H closest to zero.

In short, these results indicate that the corner edge sites have the ΔG_H that is most close to zero, and thus indicating the best catalytic activity for the hydrogen evolution. In addition, we explored the hydrogen coverage

effects by taking the ZZ-S2 model (n=6) as one example. We added 1, 3, 6, and 7 H atoms on the edge site of Se layer (the seventh H atom was added above the Se atom in the middle of the MoSSe), and calculated the changes of hydrogen Gibbs free energy (ΔG_H) with respect to the hydrogen coverage that was defined as the atomic ratio between the number of H and Se atoms in the model. As shown in Figure 5, an estimated hydrogen coverage is about 25% (H:Se) for $\Delta G_H < 0.2$ eV, and as the increase of hydrogen coverage, adsorption on the other sites (edges) is less likely to occur because of the weak adsorption interaction. This is consistent with a previous computational study on the hydrogen coverage effects on the MoS_2 surfaces.[35]

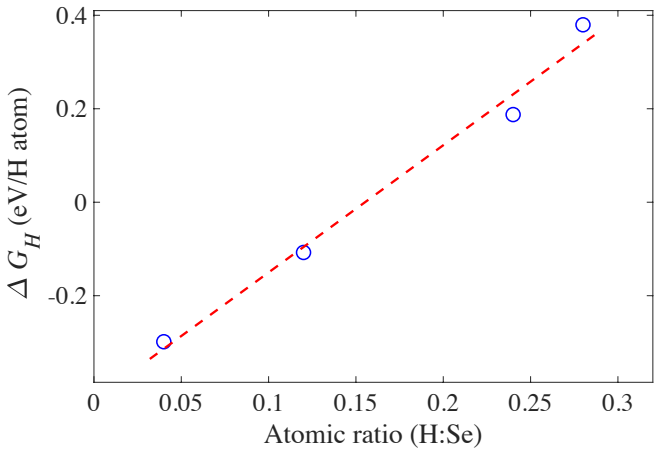

Fig. 5 Calculated changes of Gibbs free energy (ΔG_H) with respect to the H:Se atomic ratio.

Next, to explore nanosize effects on the catalytic performance in the Janus MoSSe nanosheets and meanwhile to develop a qualitative understanding of the ΔG_H at S-layer and Se-layer of MoSSe, we carried out preliminary calculations for the ΔG_H of the hydrogen adsorption at S layer and Se layer, respectively, on the edges of MoSSe nanosheets with different sizes (n). Two interesting observations were found. First, as expected, ΔG_H of hydrogen adsorption on S layer is indeed more negative than that on Se layer (about 0.2 eV for the ZZ-S2 type structure and 0.5 eV for the ZZ-S1 type structure), and the ΔG_H on the Se layer is more closes to the zero, and thus one can conclude that the Se layer of Janus MoSSe nanosheets has a better catalytic activity than the S layer. Second, as the size (n) increases, there exists an obvious odd-even oscillation for the calculated ΔG_H as the size (n) increases, indicating an odd-even effect on the hydrogen adsorption.

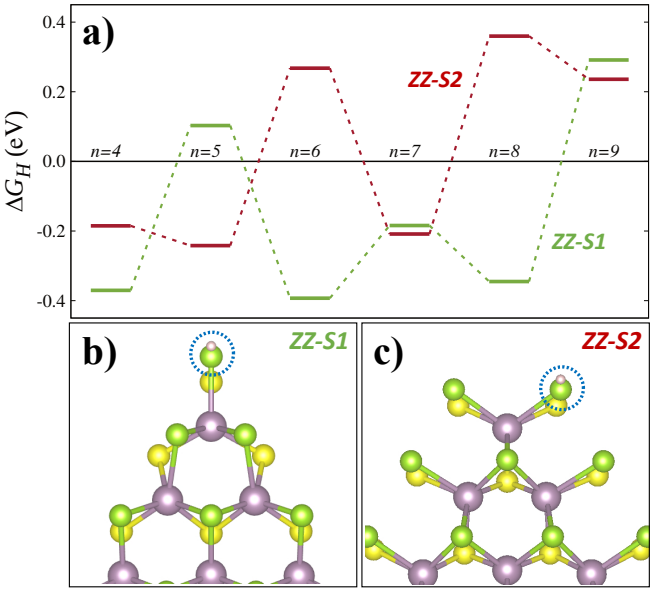

Fig. 6 a) Calculated changes of Gibbs free energies (ΔG_H) of ZZ-S1 and ZZ-S2 MoSSe nanosheets with respect to size (n). b-c) The geometrical display of the H-adsorption at the corner site for ZZ-S1 and ZZ-S2 nanosheets, respectively. The Se atoms with H adsorption are highlighted in a blue circle.

To clearly show the observed odd-even effects in the Janus MoSSe nanosheets, we plotted the calculated ΔG_H for the H adsorption on the corner edges for both ZZ-S1 and ZZ-S2 models for different sizes (n = 4-9) in Figure 6. Here the corner edges, *i.e.*, site 1 in both models (highlighted in blue), were selected based on the two considerations: i) relative low hydrogen adsorption energy and ii) ΔG_H close to zero for achieving best catalytic performance. For the ZZ-S1 model, the MoSSe nanosheets with even n's have a relatively lower ΔG_H as compared to the relatively higher ΔG_H for the odd n's. For the ZZ-S2 model, on the other hand, the calculated ΔG_H is lower at an odd n but higher at an even n, exhibiting an opposite odd-even effect to the ZZ-S1 model. In fact, an odd-even effect on the formation of sulfur vacancies has been found in the MoS_2 nanosheets because of the structural equilibrium state upon the relaxation based on the size number.[20] However, it should be noted that the odd-even effect in the asymmetrical Janus MoSSe is for the H adsorption while our previously reported odd-

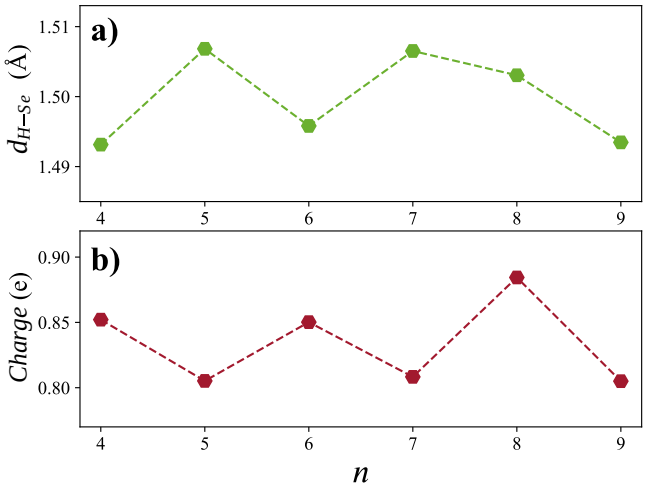

Fig. 7 Calculated H-Se bond length and the Bader charge on the Se atoms for the ZZ-S2 MoSSe nanosheet with respect to size (n).

even effects in the symmetrical MoS_2 nanosheets is for the sulfur vacancies. Therefore, in spite of the common terminology, *i.e.*, odd-even effects, the actual chemical reaction processes associated with the effects are essentially different.

The discovered odd-even effects on the hydrogen adsorption on the Janus MoSSe nanosheets can be understood from the changes of geometrical structures and the resulting charge redistribution. By taking ZZ-S2 MoSSe nanosheet as one example, we calculated H-Se bond length and corresponding charge distribution (via Bader charge analysis[36]) on the Se atom (bonded to the H atom) at different n, see Figure 7. Our calculations show an obvious odd-even effect with respect to the size (n), except at n=9, which implies that the odd-even effects may disappear for large nanostructures. The calculated Bader charge shows that Se atom (bonded to the H atom) have positive charge (Figure 7b) and adsorbed H atom has a negative charge, indicating that the charge was transferred from Se to H upon hydrogen adsorption on the MoSSe. It is worth pointing out that this is very different from other Se atoms in MoSSe where Se captures electrons from adjacent Mo atoms and serves as anions. Therefore, it is expected that the sign change of the valence state for the Se atom bonded to the H atom will cause significant charge redistribution around the Se and adjacent Mo, S, and Se atoms, thus increasing the total energy of Janus MoSSe and leading to a less stable state. At even n, a shorter H-Se bond length means a stronger H-Se bond interaction and more charge transfer from Se to H, as evidenced by the higher Bader charge on Se in Figure 7b. This also implies a higher total energy of H-adsorbed MoSSe, and thus the higher ΔG_H. In contrast, at odd n, a longer H-Se bond length leads to relatively lower Bader charge on Se, leading to a relatively lower total energy of H-adsorbed MoSSe and the resulting lower ΔG_H. The odd-even effects on the changes of H-Se bond length thus leads to same effects on the hydrogen adsorption on MoSSe.

4 Conclusions

In summary, we have studied the size effects and odd-even effects on the hydrogen adsorption in the triangular Janus MoSSe nanosheets using first-principles calculations. Our calculations indicate that these nanosheets are energetically preferred to form as the size of nanosheets increase, and these monolayer Janus MoSSe nanosheets exhibit an obvious arch structure with a bend toward S layer because of the asymmetrical layer structure. The calculated changes of Gibbs free energies (ΔG_H) of the hydrogen adsorption on the Se layers is much closer to zero than that on the S layers, thus implying a better catalytic activity. A strong odd-even effect on the hydrogen adsorption on the corner edges sites at Se layer with respect to the size (n) of the nanosheets was also found. That is, the calculated ΔG_H exhibits obvious odd-even oscillations as the size number (n) changes from odd to even.

5 Acknowledgment

Acknowledgment is made to the Donors of the American Chemical Society Petroleum Research Fund for support of this research under the award number 55481-DNI6. This work used the Extreme Science and Engineering Discovery Environment (XSEDE), which is supported by National Science Foundation grant number ACI-1548562.

References

1 H. Zhu, Y. Wang, J. Xiao, M. Liu, S. Xiong, Z. J. Wong, Z. Ye, Y. Ye, X. Yin and X. Zhang, *Nat. Nanotechnol.*, 2015, **10**, 151.

2 L. Dong, J. Lou and V. B. Shenoy, *ACS Nano*, 2017, **11**, 8242–8248.

3 L. Yang, P. Liu, J. Li and B. Xiang, *Catalysts*, 2017, **7**, 285.

4 W. Shi, K. Fan and Z. Wang, *Phys. Chem. Chem. Phys.*, 2018, **20**, 29423–29429.

5 Z. Guan, S. Ni and S. Hu, *J. Phys. Chem. C*, 2018, **122**, 6209–6216.

6 Y. Ji, M. Yang, H. Lin, T. Hou, L. Wang, Y. Li and S.-T. Lee, *J. Phys. Chem. C*, 2018, **122**, 3123–3129.

7 X. Ma, X. Wu, H. Wang and Y. Wang, *J. Mater. Chem. A*, 2018, **6**, 2295–2301.

8 Z.-K. Tang, B. Wen, M. Chen and L.-M. Liu, *Adv. Theory Simul.*, 2018, **1**, 1800082.

9 W. Shi, G. Li and Z. Wang, *J. Phys. Chem. C*, 2019, **123**, 12261–12267.

10 J. He and S. Li, *Comp. Mat. Sci.*, 2018, **152**, 151–157.

11 M. Meng, T. Li, S. Li and K. Liu, *J. Phys. D: Appl. Phys.*, 2018, **51**, 105004.

12 M. Palsgaard, T. Gunst, T. Markussen, K. S. Thygesen and M. Brandbyge, *Nano Lett.*, 2018, **18**, 7275–7281.

13 W.-J. Yin, B. Wen, G.-Z. Nie, X.-L. Wei and L.-M. Liu, *J. Mater. Chem. C*, 2018, **6**, 1693–1700.

14 J. Zhang, S. Jia, I. Kholmanov, L. Dong, D. Er, W. Chen, H. Guo, Z. Jin, V. B. Shenoy, L. Shi and J. Lou, *ACS Nano*, 2017, **11**, 8192–8198.

15 A.-Y. Lu, H. Zhu, J. Xiao, C.-P. Chuu, Y. Han, M.-H. Chiu, C.-C. Cheng, C.-W. Yang, K.-H. Wei, Y. Yang, Y. Wang, D. Sokaras, D. Nordlund, P. Yang, D. A. Muller, M.-Y. Chou, X. Zhang and L.-J. Li, *Nat. Nanotechnol.*, 2017, **12**, 744–749.

16 B. Song, L. Liu and C. Yam, *J. Phys. Chem. Lett.*, 2019, **10**, 5564–5570.

17 C. Tsai, F. Abild-Pedersen and J. K. Nørskov, *Nano Lett.*, 2014, **14**, 1381–1387.

18 A. Bruix, H. G. Füchtbauer, A. K. Tuxen, A. S. Walton, M. Andersen, S. Porsgaard, F. Besenbacher, B. Hammer and J. V. Lauritsen, *ACS Nano*, 2015, **9**, 9322–9330.

19 Q. Tang and D.-e. Jiang, *ACS Catal.*, 2016, **6**, 4953–4961.

20 P. H. Joo, J. Cheng and K. Yang, *Phys. Chem. Chem. Phys.*, 2017, **19**, 29927–29933.

21 P. H. Joo and K. Yang, *Mol. Syst. Des. Eng.*, 2019, **4**, 974–982.

22 Y.-N. Wen, M.-G. Xia and S.-L. Zhang, *Comp. Mat. Sci.*, 2018, **152**, 20–27.

23 W. Shi and Z. Wang, *J. Phys.: Conden. Matt.*, 2018, **30**, 215301.

24 J. Wang, H. Shu, T. Zhao, P. Liang, N. Wang, D. Cao and X. Chen, *Phys. Chem. Chem. Phys.*, 2018, **20**, 18571–18578.

25 R. R. Chianelli, M. H. Siadati, M. P. De la Rosa, G. Berhault, J. P. Wilcoxon, R. Bearden Jr and B. L. Abrams, *Catal. Rev.*, 2006, **48**, 1–41.

26 F. Besenbacher, M. Brorson, B. S. Clausen, S. Helveg, B. Hinnemann, J. Kibsgaard, J. V. Lauritsen, P. G. Moses, J. K. Nørskov and H. Topsøe, *Catal. Today*, 2008, **130**, 86–96.

27 S. Helveg, J. V. Lauritsen, E. Lægsgaard, I. Stensgaard, J. K. Nørskov, B. Clausen, H. Topsøe and F. Besenbacher, *Phys. Rev. Lett.*, 2000, **84**, 951.

28 J. V. Lauritsen, J. Kibsgaard, S. Helveg, H. Topsøe, B. S. Clausen, E. Lægsgaard and F. Besenbacher, *Nat. Nanotechnol.*, 2007, **2**, 53.

29 T. F. Jaramillo, K. P. Jørgensen, J. Bonde, J. H. Nielsen, S. Horch and I. Chorkendorff, *Science*, 2007, **317**, 100–102.

30 G. Kresse and D. Joubert, *Phys. Rev. B*, 1999, **59**, 1758–1775.

31 G. Kresse and J. Furthmüller, *Comp. Mat. Sci.*, 1996, **6**, 15–50.

32 P. E. Blöchl, *Phys. Rev. B*, 1994, **50**, 17953–17979.

33 J. P. Perdew, K. Burke and M. Ernzerhof, *Phys. Rev. Lett.*, 1996, **77**, 3865–3868.

34 B. Hinnemann, P. G. Moses, J. Bonde, K. P. Jørgensen, J. H. Nielsen, S. Horch, I. Chorkendorff and J. K. Nørskov, *J. Am. Chem. Soc.*, 2005, **127**, 5308–5309.

35 R. Kronberg, M. Hakala, N. Holmberg and K. Laasonen, *Phys. Chem. Chem. Phys.*, 2017, **19**, 16231–16241.

36 W. Tang, E. Sanville and G. Henkelman, *J. Phys.: Conden. Matt.*, 2009, **21**, 084204.

Graphic Abstract